Electrochemical dating of archaeological gold based on refined peak current determinations and Tafel analysis

Supplementary information

Antonio Doménech-Carbó[a], Fritz Scholz[b], Michael Brauns[c], SianTiley-Nel[d], Arturo Oliver[e], Gustavo Aguilella[f], Noemí Montoya[a], María Teresa Doménech-Carbó[g]

[a] Department of Analytical Chemistry, University of Valencia, Dr. Moliner, 50, 46100, Burjassot (Valencia), Spain
[b] Universität Greifswald, Institut für Biochemie, Felix-Hausdorff Straße 4, 17487, Greifswald, Germany
[c] Curt-Engelhorn-Zentrum Archäometrie gGmbH, D6,3 (OG 3), 68159, Mannheim, Germany
[d] Faculty of Humanities, Department of Historical and Heritage Studies, University of Pretoria & University of Pretoria Museums, Old Arts Building University of Pretoria, Private Bag X20, Hatfield, 0028, South Africa
[e] Museu de Belles Arts de Castelló, Avenida Hermanos Bou, 28, 12003, Castellón de la Plana, Spain
[f] Servicio de Investigaciones Arqueológicas y Prehistóricas, Diputación de Castellón Avda, Hnos Bou 28 (edificio Museu), 12003, Castellón, Spain
[g] Institut de Restauració del Patrimoni, Universitat Politècnica de València, Camí de Vera 14, 46022, València, Spain

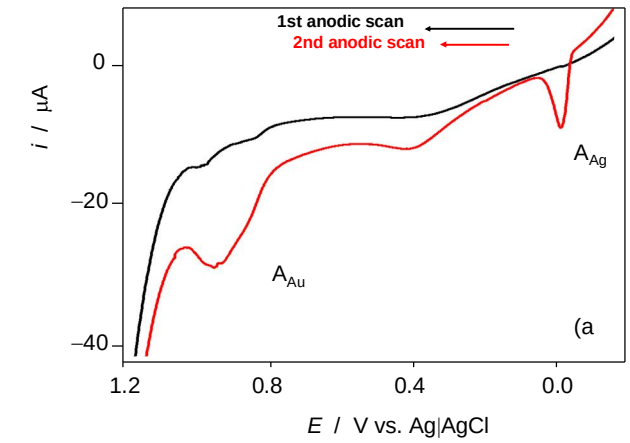

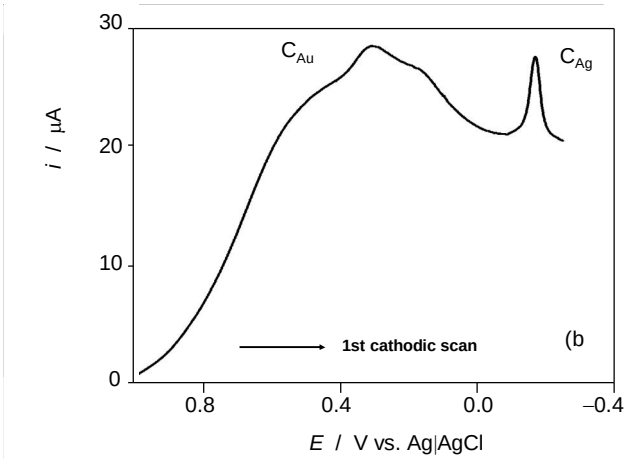

Figure S.1. Illustration of the sequence anodic – cathodic –anodic LSVs used in the study of archaeological gold samples. a) First (black line) and second (red line) anodic LSVs and b) first cathodic scan performed after the initial anodic one of the Santa Llúcia sample SL01 attached to graphite electrode in contact with air-saturated 0.10 M HCl. Potential scan rate 50 mV s^{-1}. The arrows indicate the direction of the potential scan.

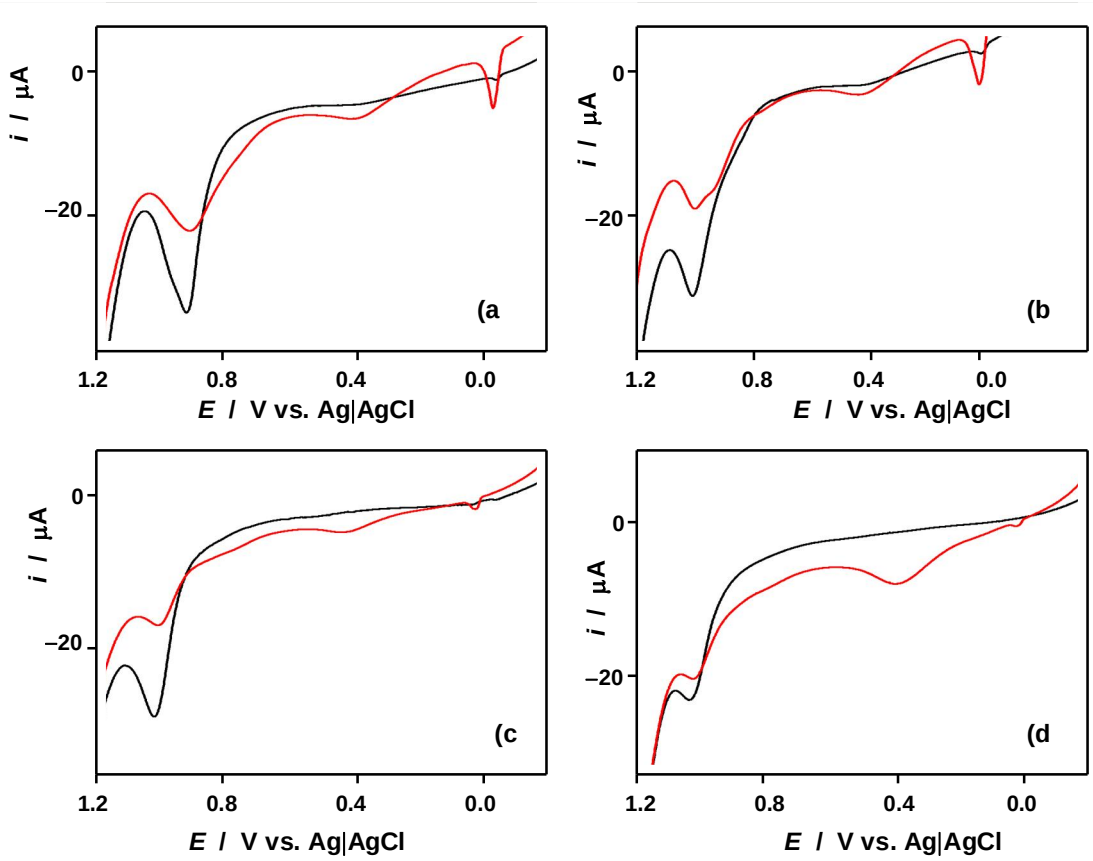

Figure S.2. First (black line) and second (red line) anodic LSVs of samples a) SL02; b) SL04; c) MU02; d) MU03 attached to graphite electrode in contact with air-saturated 0.10 M HCl. Potential scan rate 50 mV s^{-1}.

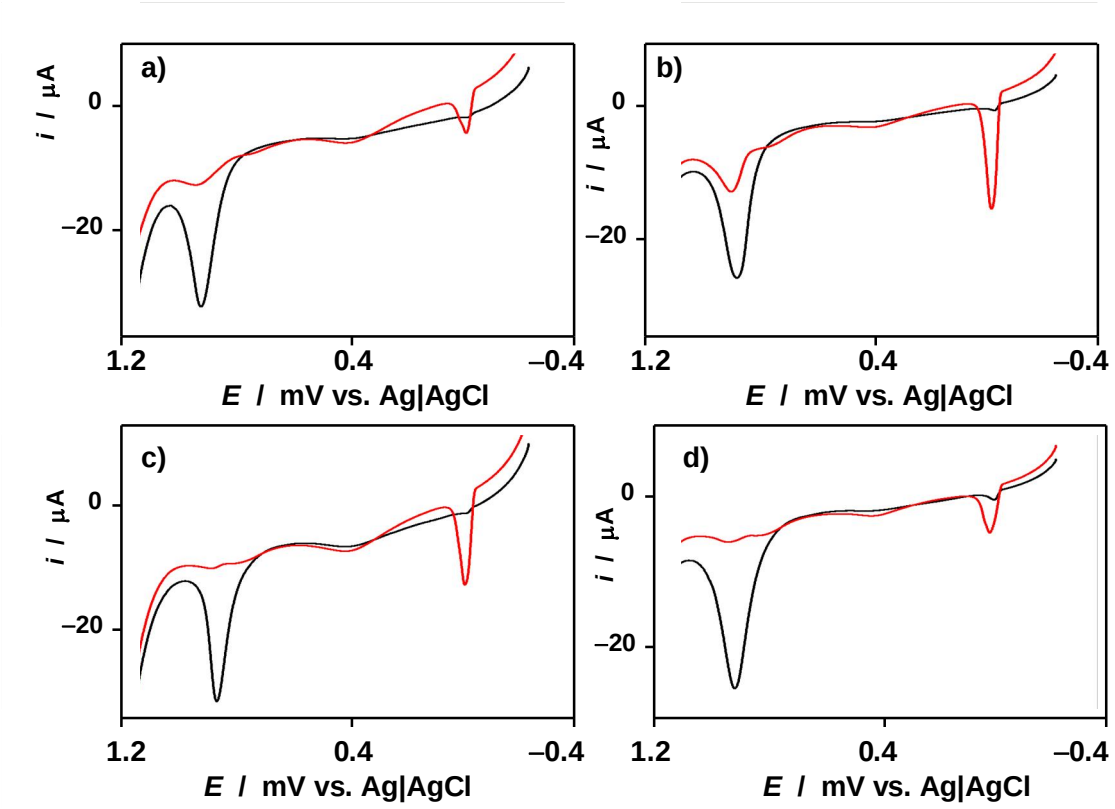

Figure S.3. First (black line) and second (red line) anodic LSVs of samples a) MA09; b) MA11; c) MA08; d) Z01 attached to graphite electrode in contact with air-saturated 0.10 M HCl. Potential scan rate 50 mV s^{-1}.

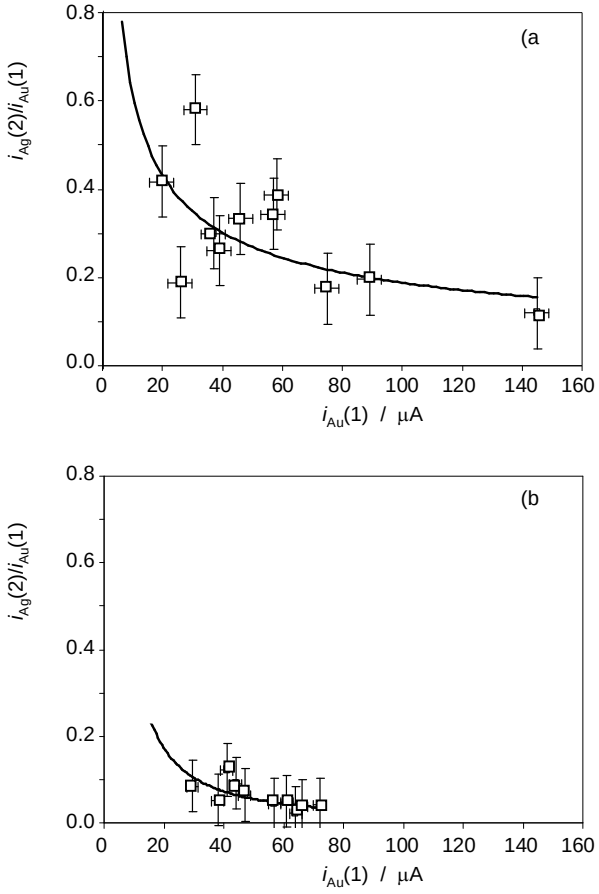

Figure S.4. Plots of the $i_{Ag}(2)/i_{Au}(1)$ ratio, representative of the bulk Ag/Au composition, with $i_{Au}(1)$ for a) Mapungubwe (1200-1250 CE) and b) Santa Llúcia (700 BCE) samples in this study. From voltammetric data such as in Fig. 1.

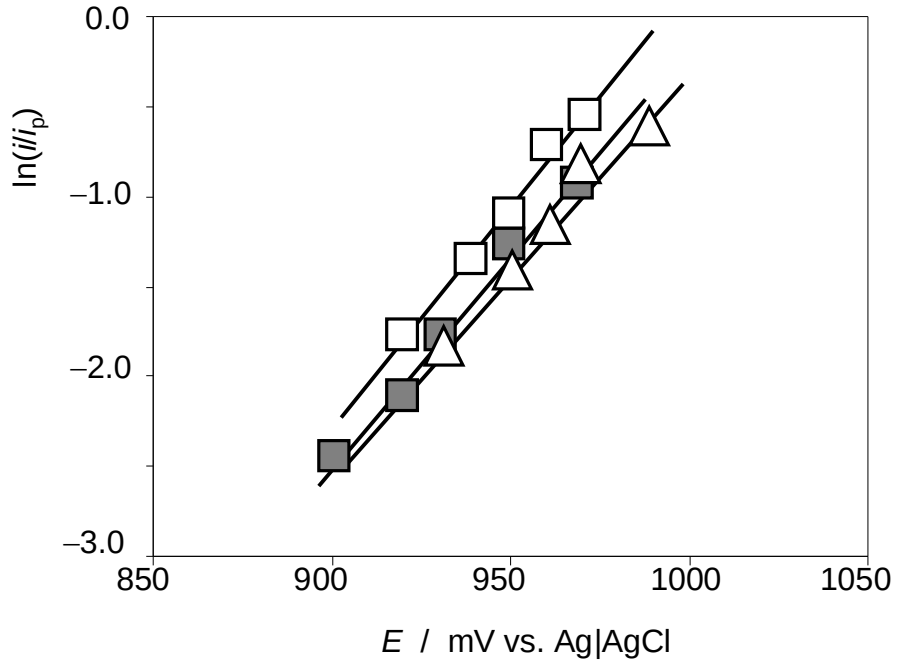

Figure S.5. Tafel plots of the logarithm of the ratio between the current *i* at a given potential E and the peak current in the voltammogram, i_p (ln(i/i_p)), vs. *E* for three replicate experiments on Mapungubwe sample MA05. Data from the rising portion of the voltammetric wave $A_{Au}(1)$ recorded in voltammograms such as in Fig. 1.

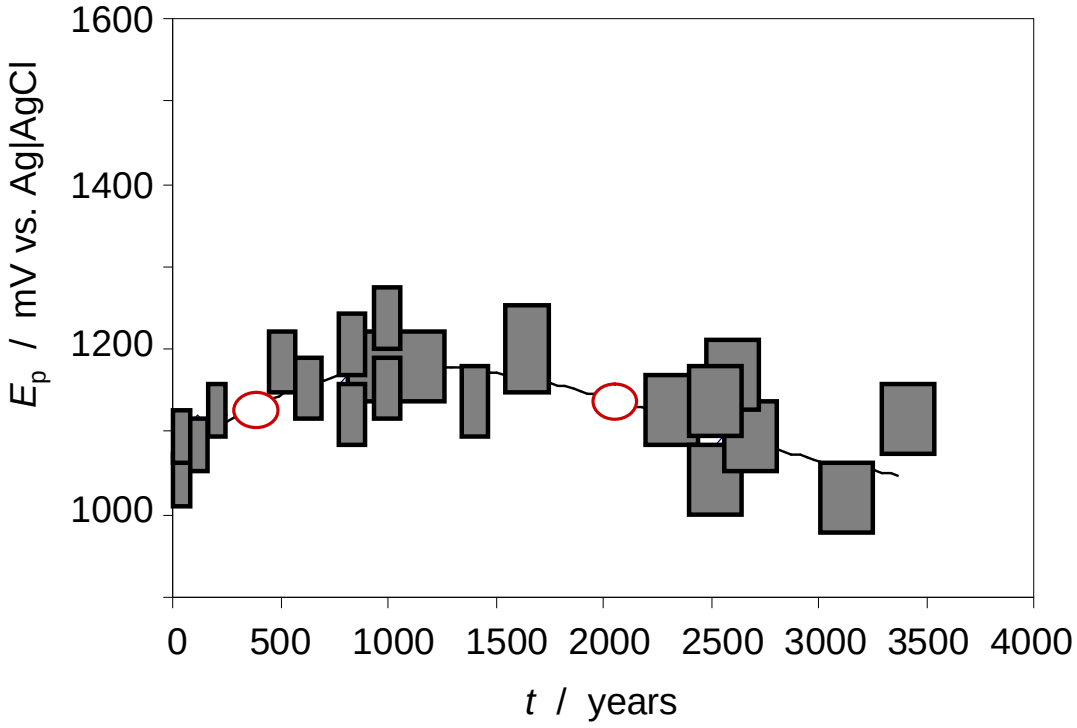

Figure S.6. Calibration graph for age determination based on uncorrected E_p; measurements using voltammetric data such as in Fig. 1. The circles mark the possible positions of problem sample MA01. This representation is similar to that in Figure 10a, but the uncorrected potentials depicted here show higher dispersion than the corrected ones.

Table S.1. Statistical parameters for the Tafel analysis of voltammetric waves $A_{Au}(1)$ recorded for selected gold samples in this study. From LSVs such as in Figure 1. [a] *SL* denotes the slope ; [b] *OO* denotes the ordinate at the origin in the Tafel plots of the representation of $\ln(i/i_p)$ vs. *E* for the rising portion of the voltammetric peak $A_{Au}(1)$ taking the base line depicted in Figure 1.

Sample	E_p **(mV vs. Ag/AgCl)**	***SL*[a]**	***OO* (mV vs. Ag/AgCl)[b]**	***r***	E_{ccp} **(mV vs. Ag/AgCl)**
Z03	930	0.0388±0.0017	−34.7±1.5	0.9990	977±60
Z03	935	0.0429±0.0008	−38.9±0.8	0.9998	979±50
Z03	930	0.0364±0.0009	−32.6±0.8	0.9997	987±60
MU05	1040	0.0228±0.0014	−23.0±1.3	0.994	1174±70
MU05	1055	0.0256±0.0013	−25.3±1.2	0.996	1198±70
MU05	1040	0.0223±0.0018	−22.6±1.7	0.991	1210±70
SL05	1040	0.0180±0.0003	−17.7±0.2	0.9998	1265±60
SL05	1020	0.0137±0.0012	−13.6±1.1	0.996	1306±80
SL05	1030	0.0146±0.0015	−14.6±1.4	0.994	1290±80